Fracture initiation revealed by variations in the fatigue fracture morphologies of PA 66 and PET fibers

J. M. HERRERA RAMIREZ, A. R. BUNSELL
Ecole des Mines de Paris, Centre des Matériaux, B.P. 87, 91003 Evry Cedex, France

The tensile and fatigue fracture morphologies of polyamide 66 (PA 66) and polystyrene (PET) fibers are well known [1]. Tensile, and also creep, failure in both fibers is similar and generally involves crack initiation at or near the fiber surface, followed by slow crack propagation, as shown in Fig. 1 [2].

Tensile failure occurs when the remaining cross section can no longer support the induced stress and rapid failure occurs, giving the type of failure morphology shown in Fig. 2.

Crack propagation under conditions which induce fatigue in these fibers is markedly different from tensile failure. In both fibers, crack initiation is, usually, as in monotonic tension, at or near the surface. However, under fatigue conditions the crack propagation is deviated so as to run at a slight angle to the fiber axis, gradually reducing the load bearing cross section [3]. Complementary broken ends of a PA 66 fiber broken in fatigue are shown in Fig. 3. It can be seen from Fig. 3 that the one broken end consists of a long tongue of material, the free end of which is the point of crack initiation. It can be noted that the tongue is always curved inwards towards the fiber axis, suggesting a residual compressive stress in the surface of the formally intact fiber. A closer inspection of the tongue shows that the fatigue fracture surface is concave, with respect to the fiber surface and not convex as would be expected if a pealing mechanism was driving crack propagation [4]. The complimentary end reveals the reduction of the load bearing section and both areas of final failure show that the final stage of fracture is by the tensile process shown above.

Fatigue failure in PET fibers occurs under similar cyclic conditions to those which produce fatigue failure in PA 66, but the angle of crack penetration is smaller so that longer tongues are generally seen and final failure occurs often behind the fatigue crack tip by a creep process.

In both tensile and fatigue failure the process of crack initiation is poorly understood, though some fracture morphologies seem to indicate the role of a thin surface layer on some fibers or the presence of an irregularity at the point of initiation. The present study has identified several unusual fracture morphologies, which have been induced under conditions which were known to provoke fatigue failure. The slower crack propagation which occurs during the fatigue process has allowed the causes of the initiation of some cracks to be determined. It is thought that these observations may be of relevance in the understanding of crack initiation in both tensile and fatigue failure.
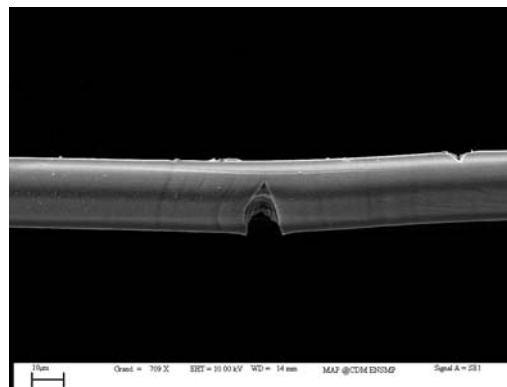
Figure 1 Slow crack growth from the surface of a PA 66 fiber under monotonic tensile loading.
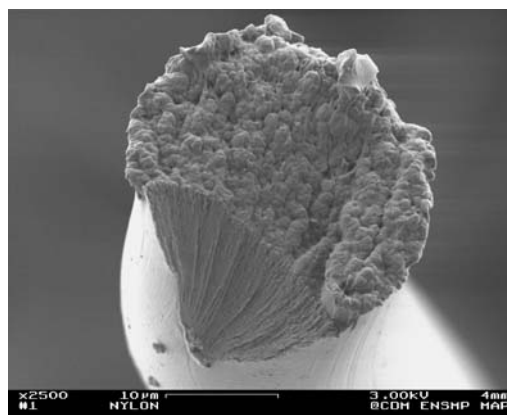
Figure 2 Typical monotonic tensile fracture morphology of a PA 66 fiber.

Figure 3 Typical fatigue fracture morphology of a PA 66 fiber.
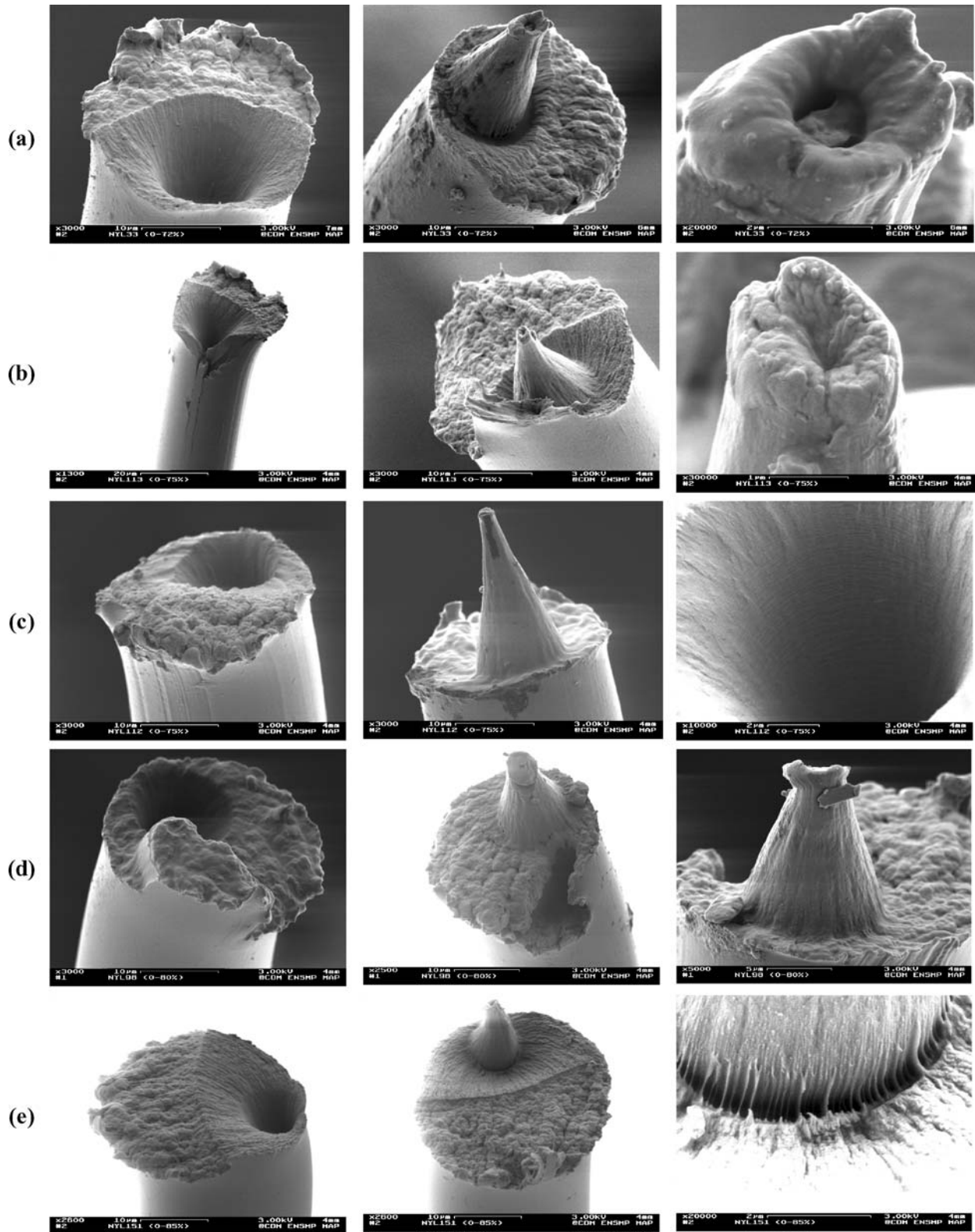
Figure 4 SEM micrographs of PA 66 fibers. (a, b and c) Fibers tested at 0–75% σ_R and broken after 201 600, 1.05×10^6 and 2.01×10^6 cycles, respectively. (d) Fiber tested at 0–80% σ_R after 554 400 cycles. (e) Fiber tested at 0–85% σ_R after 437 400 cycles.

The specimens which have been tested have been industrially produced high tenacity PA 66 and PET monofilaments, which have been subjected to fatigue tests in a universal fiber tester [5] under controlled conditions of relative humidity and temperature (50% and 21 °C). The fibers were sinusoidally cycled at 50 Hz from zero load to a maximum load which was varied from 75 to 85% of the fiber's simple tensile strength (σ_R). It had previously been ascertained that the fibers consistently failed with the fatigue fracture morphology under these loading conditions. The broken ends of the fibers were subsequently examined in a field effect scanning electron microscope (SEM), which was equipped with an energy dispersive spectrometer (EDS) microanalysis system.
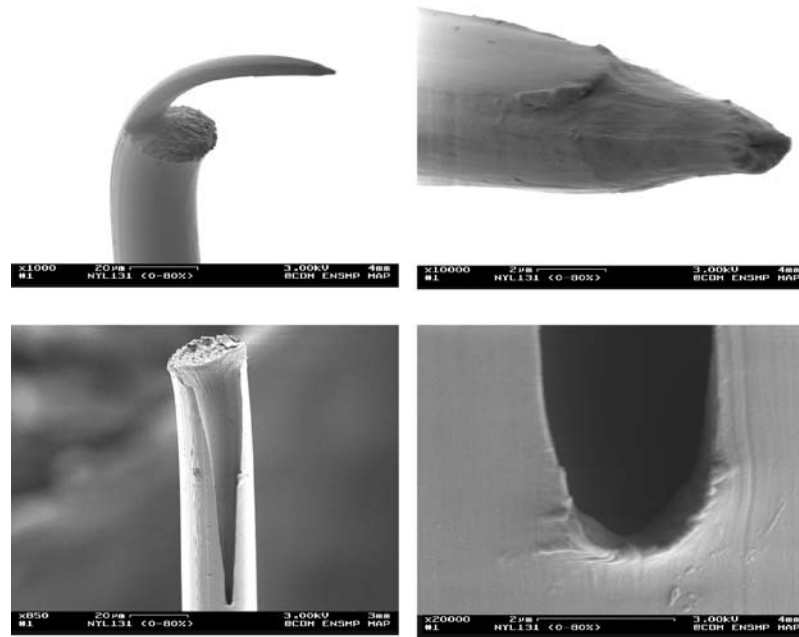
Figure 5 SEM micrographs of a PA 66 fiber tested at 0–80% σ_R and broken after 894 600 cycles.

The SEM observations revealed that most of the fibers broke as in Fig. 3. However, some fibers presented very particular fracture morphologies, as it can be seen from the four fiber failures shown in Fig. 4.

One end of each fracture end can be seen to consist of a large cavity, which blends into the two regions of slow and rapid crack growth as seen in tensile and creep failures. The complimentary ends show a cone of material the apex of which can be seen not to be a point but rather a crater, in which, in some cases, a particle may be seen to be lodged. These fracture morphologies indicate that, unusually, the fatigue cracks have been initiated at a point inside the fibers and that the slow crack growth at a slight angle to the fiber axis has produced the conical morphology which, when the cross section was sufficiently reduced, led to tensile failure. The advance of the fatigue crack front is shown by regular striations on the inside surface of the conical cavity, most clearly seen in Fig. 4c. The transition from fatigue to tensile failure can be seen in Fig. 4e to be marked by the presence of macrofibrils which bridge the two regions.

Fig. 5 shows another PA 66 fiber tested at 0–80% σ_R and broken after 894 600 cycles. The appearance of this fiber break is similar to a standard fatigue failure, however it can be clearly seen that crack initiation took place within the body of the fiber, though near the surface and that the top of the tongue presents a similar morphology to the fibers shown Fig. 4.

Fig. 6 shows complementary ends of a PET fiber tested at 0–85% σ_R and which broke by a creep process, after 4.22×10^6 cycles. A particle of about 1.5 μm can be seen to be at the point of crack initiation and a complementary crater observed in the complementary fracture surface. The size of the particle corresponded approximately to the craters at the end of the conical fracture ends seen in some PA 66 fibers and shown in Fig. 4.

An EDS semi quantitative microanalysis was carried out in order to identify the nature of the particle, as shown in Fig. 7. The result showed that antimony and phosphorus or zirconium were present in the particle.

It is not usually possible to observe, with a scanning electron microscope, deep inside the conical hole on the one side of the break, but it was thought likely that any particle which might have been the cause of the failure initiation could remain lodged at this point. The break was therefore observed with a light transmission
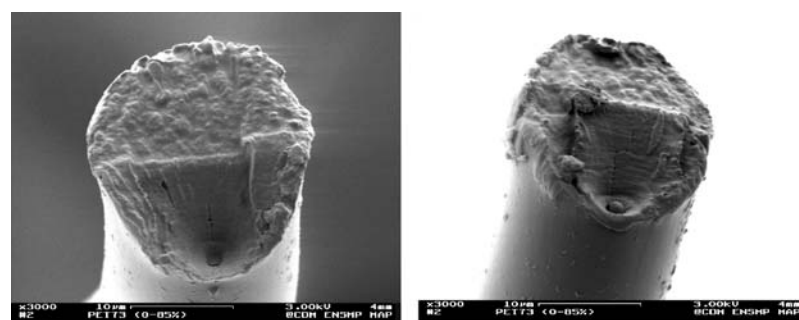
Figure 6 SEM micrographs of a PET fiber tested at 0–85% σ_R and broken after 4.22×10^6 cycles.
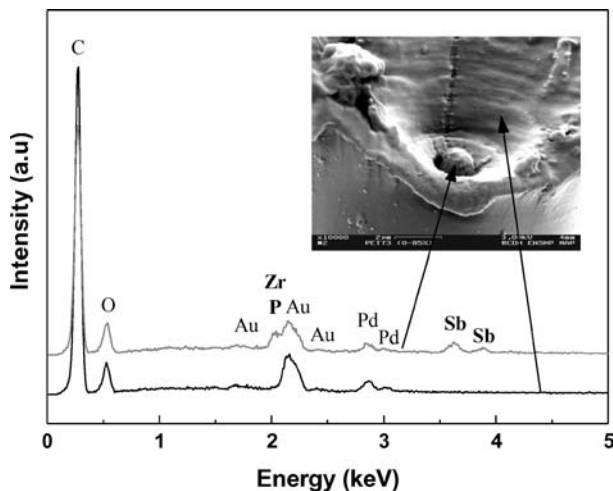
Figure 7 EDS microanalysis results from the PET fiber.
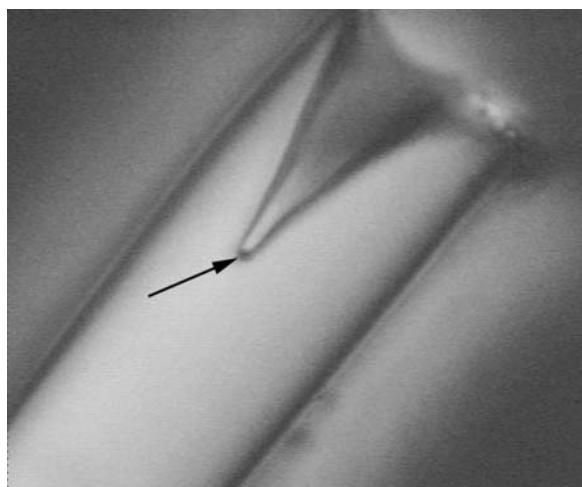
Figure 8 Optical micrograph showing a particle at the bottom of a cavity in a PA66 fiber.

optical microscope equipped with a polarizer stage. Fig. 8 shows that a particle can be observed, as indicated by the arrow, deep inside a PA66 fiber. It is at the initiation site of the failure and confirms it as being the cause of initial failure. Such particles were not observed at the tip of all the breaks and it is supposed that in some cases the particle is lost at the moment of failure.

These observations reveal that the initiation of failure in both PA 66 and PET fibers can be due to the presence of foreign bodies which in the case of PET fibers is likely to be antimony trioxide (Sb_2O_3) used as a catalyst in the production of the polymer. The fatigue processes in the PA 66 fibers discussed can be seen also to have originated most probably at similar particles, though not necessarily of antimony. In many PA 66 fibers, particularly for textile applications, TiO_2 is added and could be the cause of crack initiation. The conical shape of the fatigue fracture is to be compared with the fracture more normally observed in fatigue
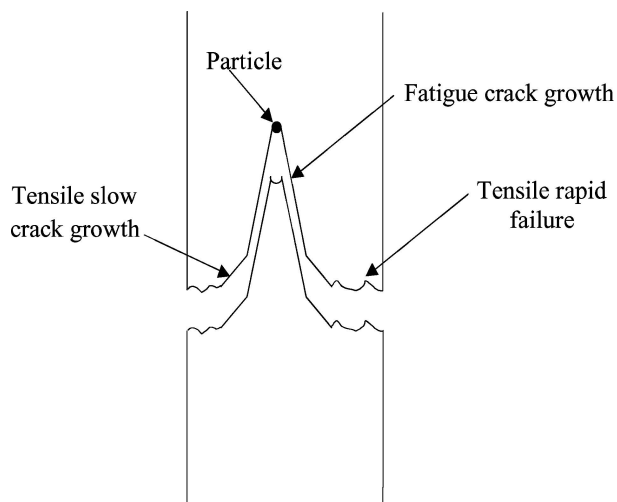
Figure 9 Schematic view of the crack propagation processes which produce the cone-shaped fatigue failures.

in which the fracture surface is concave to the outside surface, unlike the convex fracture surface which is circumferential in shape, obtained by peeling the fibers. Fig. 9 shows schematically the steps in crack propagation which produce this type of failure.

The failure processes of PA 66 and PET fibers are very similar, both in tension and fatigue. The failure shown in Fig. 6 of a PET fiber shows that it failed in creep, during cyclic loading and that the crack was initiated by the presence of a particle, probably of antimony. Fig. 8 shows that a similarly sized particle initiated fatigue failure in the PA66 fiber which is shown.

These observations have revealed that the controlled development of fatigue cracks can be used to identify the causes of failure in fibers and that the causes, in fatigue and also in tension and creep can be the presence of particles. These particles could be foreign bodies which have inadvertently found their way into the production process but most likely are used, deliberately in the production process. Closer control of the granulometry of these materials could improve fiber properties.

References
1. J. W. S. HEARLE and P. M. CROSS, *J. Mater. Sci.* **5** (1970) 507.
2. A. MARCELLAN, Ph.D Thesis, Ecole Nationale Supérieure des Mines de Paris, 2003.
3. A. R. BUNSELL and J. W. S. HEARLE, *J. Appl. Polym. Sci.* **18** (1974) 267.
4. CH. OUDET and A. R. BUNSELL, *J. Mater. Sci.* **22** (1987) 4292.
5. A. R. BUNSELL, J. W. S. HEARLE and R. D. HUNTER, *J. Phys.* E **4** (1971) 868.